

EVALUATION OF $\text{Al}_x\text{Ga}_{1-x}\text{As}$ SOLAR CELLS

R.Y. Loo, G.S. Kamath, R.C. Knechtli, and A. Narayanan
Hughes Research Laboratories
Malibu, California

S.S. Li
University of Florida
Gainesville, Florida

Single junction GaAs solar cells have already attained an efficiency of 19% AMO which could potentially be increased to ~20 %, with some optimization. To achieve the higher efficiency we must employ the concept of multibandgap solar cells which utilizes a wider region of the solar spectrum. One of the materials for fabricating the top cell in a multibandgap solar cell is AlGaAs because it is compatible with GaAs in bandgap and lattice match. This is a very important consideration from the materials technology point of view; this paper evaluates the viability of this approach. It is interesting to note that in this context the technology for AlGaAs has been well developed for applications to lasers and to high speed transistors.

AlGaAs LPE GROWTH

During the past few years we have developed and perfected the infinite solution LPE growth technique for the fabrication of single junction GaAs solar cells. We are now extending the technology to the fabrication of AlGaAs solar cells. Since Al is a very reactive element and is easily oxidized when exposed to air, we need to grow two AlGaAs layers in succession on a GaAs substrate. To achieve this goal we modified the crucible in our LPE furnace to a multiwell crucible using different AlGaAs solutions, including the p-type AlGaAs solution with Be as the dopant. The other solutions are n-type, Sn-doped $\text{AlGa}_{1-x}\text{As}$ solutions. Figure 1 shows a sketch of our multiwell crucible and Table I indicates the composition of each solution. Figure 2 shows the baseline design of an AlGaAs solar cell; it is identical to our AlGaAs-GaAs homojunction solar cell. Figure 3 shows the entire temperature cycle for growing the AlGaAs solar cell from a multiwell system. The first layer is an n-type AlGaAs base layer grown directly on a GaAs substrate and the second layer is the p-type AlGaAs window layer. The AlGaAs window layer is necessary to reduce the surface recombination velocity at the front surface of the cell. During the growth of the window layer, the dopant (Be) diffuses into the base n-AlGaAs layer to form an active photovoltaic junction.

RESULTS AND DISCUSSIONS

We have fabricated a number of AlGaAs solar cells with three different Al concentrations in the base region of the cell. Figures 4, 5, and 6 show the photo IV and spectral response of these cells. Table II summarizes the results from these measurements. The short circuit currents measured from these cells are lower than expected for the Al concentration in the base layer. The reduction in the cell's short circuit current is not caused solely by the increase of the bandgap in the material as the Al concentration is increased. In our experimental cells made to date, this loss of short circuit current was caused to a large extent by decreased electrons and hole diffusion lengths, combined with an excessive junction depth.

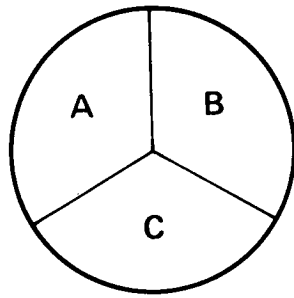
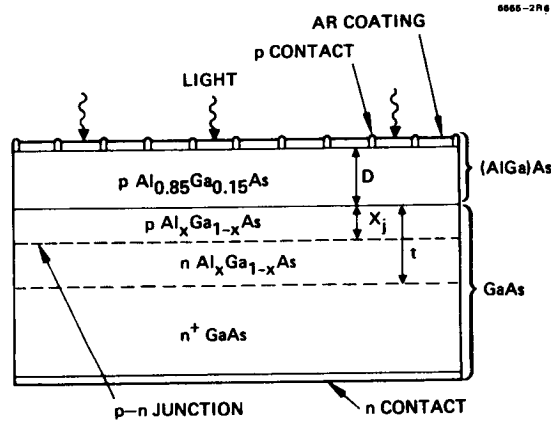


Figure 1. Multiwell crucible (top view) for growing $\text{Al}_x\text{Ga}_{1-x}\text{As}$.



NUMBER OF FINGERS = 24

p CONTACT: Au-Zn-Ag

n CONTACT: Au-Ge-Ni-Ag

AR COATING: Ta_2O_x

CELL SIZE = 2 cm x 2 cm

Figure 2. $\text{Al}_x\text{Ga}_{1-x}\text{As}$ solar cell structure.

Table I. Melt Composition in the Multiwell Crucible

<u>Melt</u>	<u>Melt Size</u>	<u>Solution</u>	<u>Type</u>
A	1500 g	$\text{Al}_{0.85}\text{Ga}_{0.15}\text{As}$	p^+ (Be)
B	1500 g	$\text{Al}_x\text{Ga}_{1-x}\text{As}$	n (Sn)
C	1500 g	$\text{Al}_x\text{Ga}_{1-x}$	n (Sn)

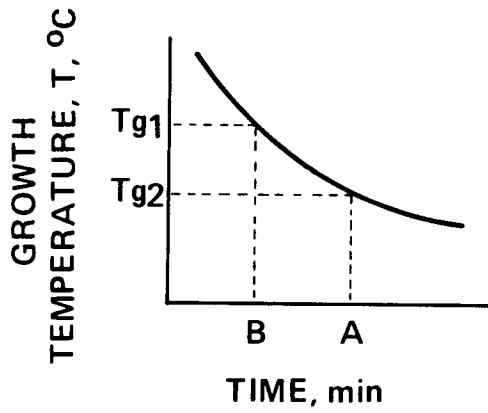


Figure 3. Temperature cycle for growing $\text{AlGa}_{1-x}\text{As}$ (growth sequence: 1 B \rightarrow 2 A).

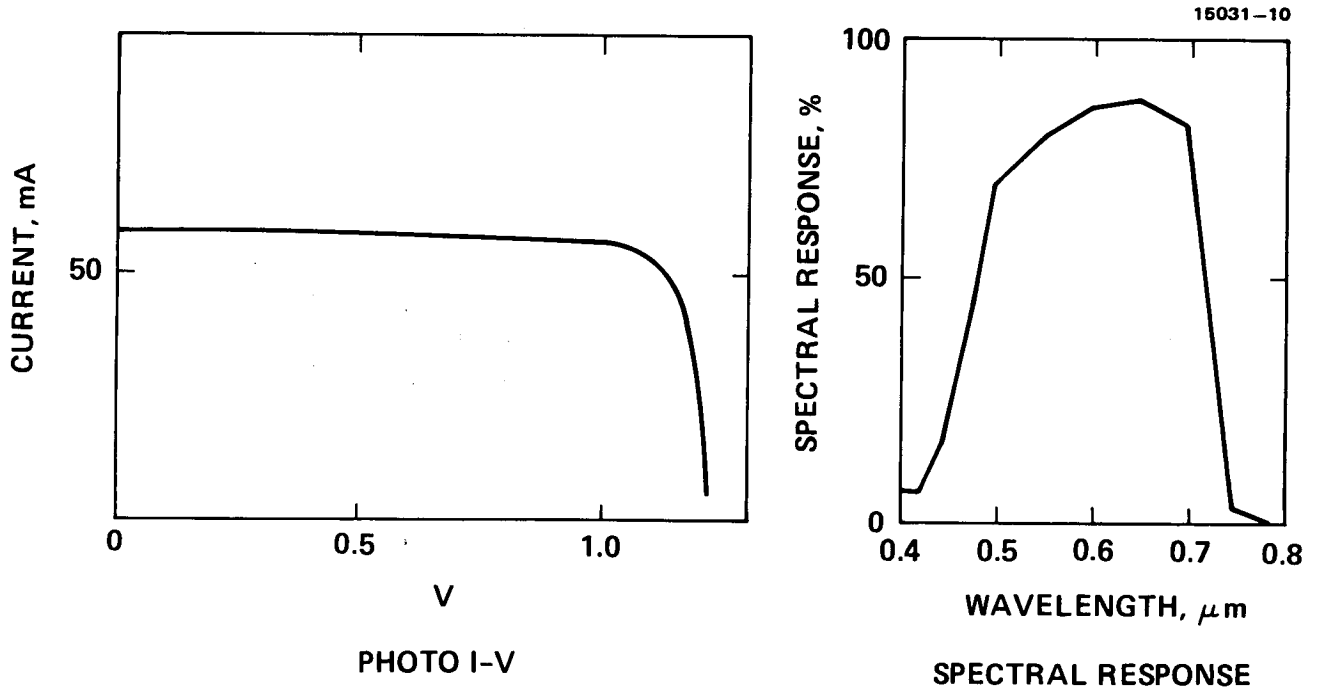


Figure 4. AlGaAs solar cell characteristics (Al concentration = 20%; cell area, 2 cm x 2 cm).

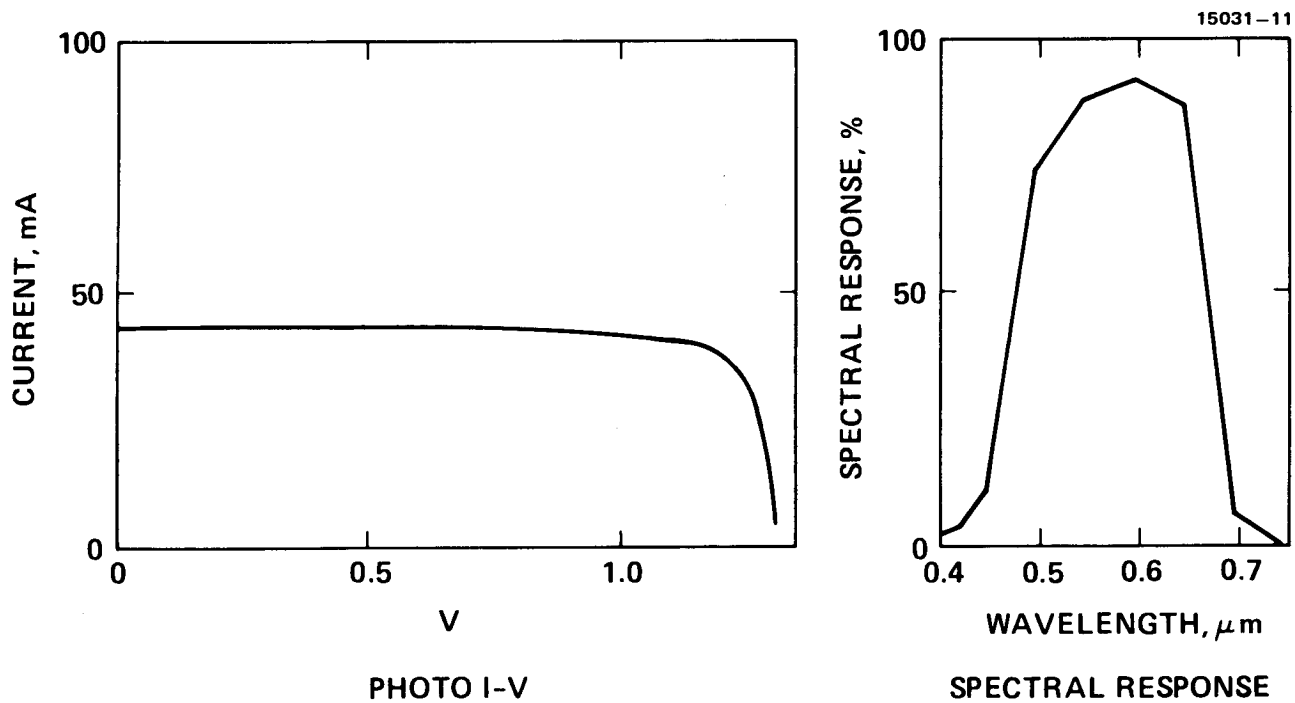


Figure 5. AlGaAs solar cell characteristics (Al concentration = 30%; cell area, 2 cm x 2 cm).

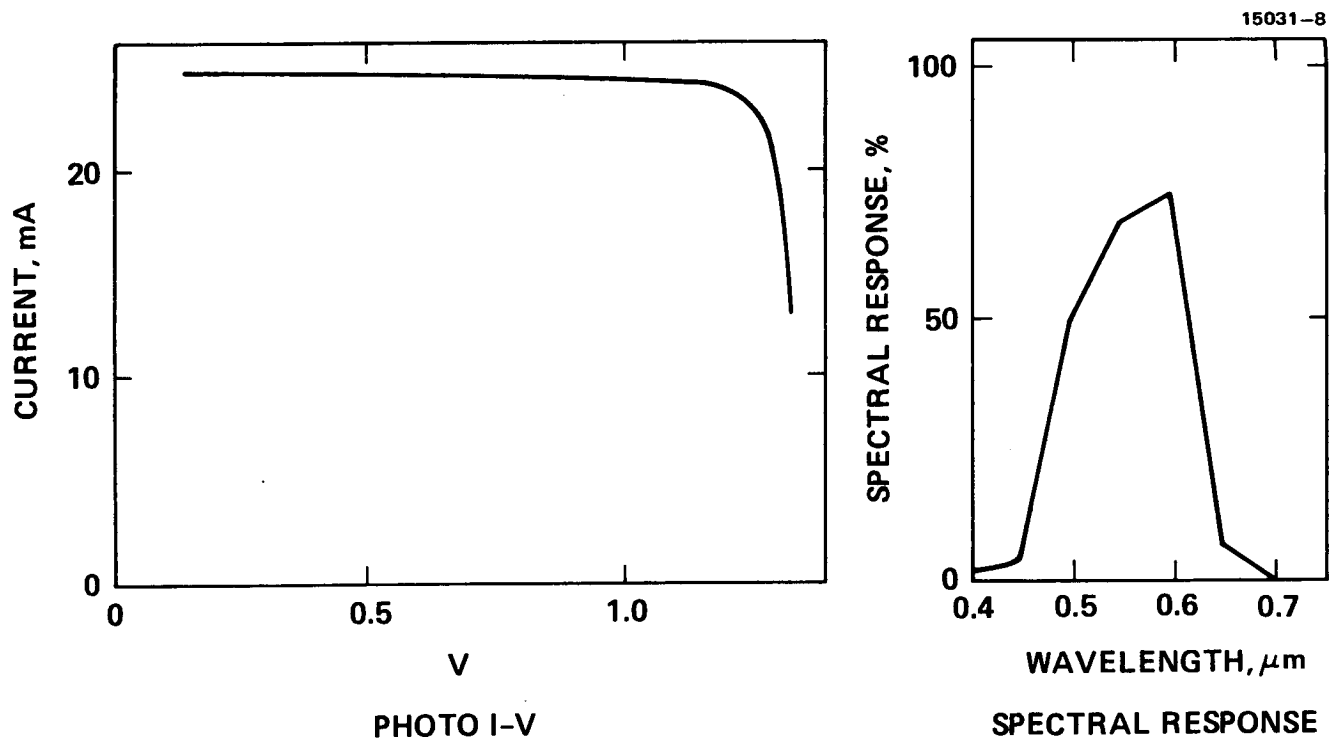


Figure 6. AlGaAs solar cell characteristics (Al concentration = 40%; cell area, 2 cm x 2 cm).

Table II. Al_xGa_{1-x}As Solar Cell Performance (cell area, 2 cm x 2 cm)

Al CONCENTRATION %	I _{SC} mA	V _{OC} V	FF	P _{MAX} mW	η %
20	59.0	1.22	0.810	58.32	10.77
30	43.0	1.31	0.800	44.84	8.3
40	25.5	1.34	0.864	29.52	5.45

Figure 7 shows the measured Hall electron mobility as a function of Al concentration. The mobility is reduced from close to 2000 to 550 cm² v⁻¹ s⁻¹ when the Al concentration is increased from 20 to 40 %. The decrease in mobility is due to the Al alloy composition in the materials. The lower value of mobility reflects lower diffusion lengths since diffusion length is related to the mobility by $L = ((kT/q) * \tau)^{1/2}$. In addition, AlGaAs may be heavily compensated in our layers. The reason for such a high compensation level is due to the increase of the impurity activation energy when the Al concentration is increased. Since solar cells require high doping density, we had to add more Sn to the AlGaAs solution, which may also adversely affect the electrical properties of the material. In addition to the Hall mobility, the lifetime of the minority carriers can also be shortened, resulting in the observed lower diffusion length. Thus, we believe that the mobility and lifetime limitations are the main reasons for the lower performance of the cells. Use of dopants such as Te or Se may reduce the problem, but their behavior in AlGaAs needs to be carefully evaluated.

Many small area (1.6E-4 cm⁻²) AlGaAs mesa diodes identical to the structure of the large area AlGaAs solar cells described above were fabricated for Deep Level Transient Spectroscopy (DLTS) measurements to detect the defect levels as a function of Al concentration in the AlGaAs material. Figures 8 and 9 show DLTS scans of electron traps in AlGaAs material for two different Al concentrations, x = 0.2 and x = 0.3, respectively. However, we did not observe any defects in our LPE GaAs epilayers. Table III summarizes the DLTS results of the measured defect parameters in AlGaAs. The measured activation energies of electron traps for both materials are different. For the Al_{0.2}Ga_{0.8}As sample, the activation energies are 0.2 and 0.44 eV below the conduction band, while the activation energies of electron traps for the Al_{0.3}Ga_{0.7}As sample are 0.18 and 0.28 eV below the conduction band. The difference in the activation energy of the deeper electron trap observed in these two samples may be attributed to the different DX center formed in these two samples. For example, Lang and Logan (1) have observed the E_c-0.43 eV level in the Te-doped AlGaAs specimen, while Zhou et al. (2) and Kumagai et al. (3) have observed an E_c-0.44 eV electron trap in the Si-doped AlGaAs material. Thus, the E_c-0.44 eV electron trap observed in AlGaAs material could be attributed to either the Si-impurity or the Te-impurity related defect center formed in these layers. According to Lang and Logan, this impurity center is in fact a donor and a vacancy defect complex known as a DX center. Further, Kumagai et al. have shown that the activation energies of the DX centers with group IV impurities become shallower as the mass number of impurities is increased, while those with group VI impurities remain constant. Our result is consistent with those reported by Kumagai et al. and Lang and Logan.

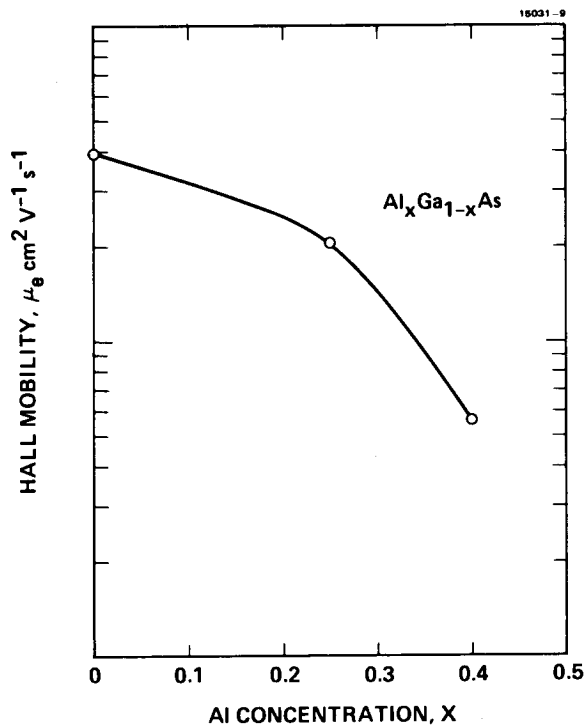


Figure 7. Electron Hall mobility, μ_e , as a function of alloy composition, x , for $\text{Al}_x\text{Ga}_{1-x}\text{As}$ alloys.

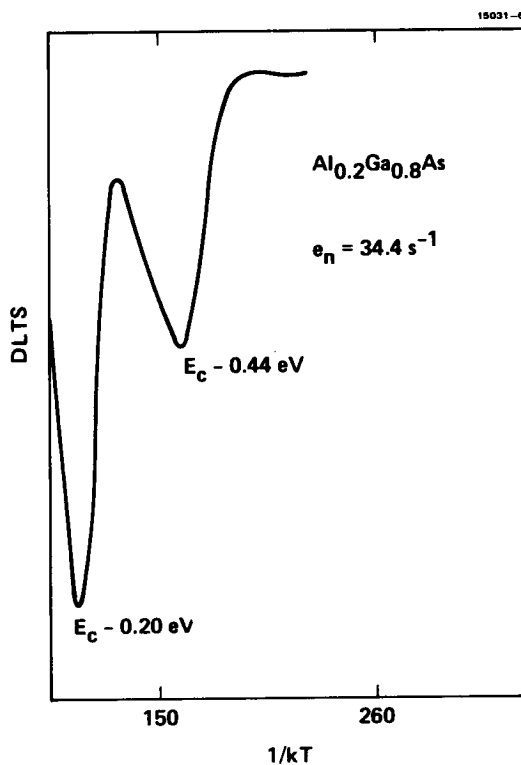


Figure 8. DLTS scan of electron traps in $\text{Al}_{0.2}\text{Ga}_{0.8}\text{As}$.

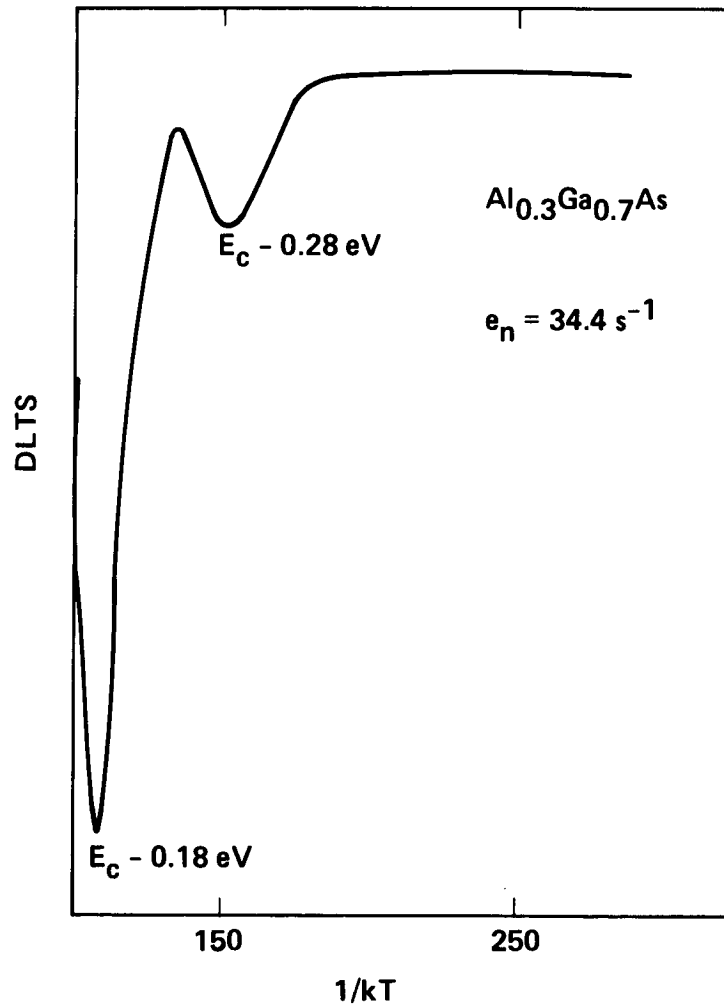


Figure 9. DLTS scan of electron traps in $\text{Al}_{0.3}\text{Ga}_{0.7}\text{As}$

Table III. Defect Parameters of $\text{Al}_x\text{Ga}_{1-x}\text{As}$ as Determined by DLTS Measurements for $x = 0.2$ and 0.3

(AREA = $4.153 \times 10^{-4} \text{ cm}^2$)	$N_D \text{ (cm}^{-3}\text{)}$	$E_T \text{ (eV)}$	$N_T \text{ (cm}^{-3}\text{)}$	$\sigma_n \text{ (cm}^2\text{)}$
$\text{Al}_{0.3}\text{Ga}_{0.7}\text{As}$	7.01×10^{16}	$E_C - 0.18$	5.70×10^{16}	6.89×10^{-15}
		$E_C - 0.28$	7.92×10^{15}	8.00×10^{-15}
$\text{Al}_{0.2}\text{Ga}_{0.8}\text{As}$	2.92×10^{17}	$E_C - 0.20$	3.10×10^{16}	
		$E_C - 0.44$	9.83×10^{15}	

SUMMARY

In summary, we have fabricated a number of AlGaAs solar cells using our LPE growth technique, and also two sets of AlGaAs mesa diodes with different Al concentrations. The AlGaAs solar cell efficiency decreases as the Al concentration is increased. We attribute the observation to the shortened diffusion length, which in turn is caused by the low electron and hole mobilities and also the lower minority carrier lifetime. This is verified by both the Hall measurements and DLTS studies on the AlGaAs materials. Our study is consistent with earlier studies by other workers; the defect centers are related to the defect complex formed by an impurity and a vacancy. We are studying methods to limit the number of these defect centers in order to improve the AlGaAs solar cell performance by optimizing the Al concentration and different dopants and dopant concentrations to reduce the problem caused by the amphoteric nature of tin.

REFERENCES

1. Land and Logan, Phys. Rev. Lett. 39, 635 (1977).
2. Zhou et al., Appl. Phys. A 28, 223 (1982).
3. Kumagai et al., Appl. Phys. Lett. 45, 1322 (1984).